JB Accepted Manuscript Posted Online 22 May 2017
J. Bacteriol. doi:10.1128/JB.00253-17

Transcriptional control of the lateral-flagellar genes of *Bradyrhizobium diazoefficiens*

Elías J. Mongiardini, J. Ignacio Quelas, Carolina Dardis, M. Julia Althabegoiti, Aníbal R. Lodeiro[#]

Instituto de Biotecnología y Biología Molecular (IBBM). Facultad de Ciencias Exactas, Universidad Nacional de La Plata y CCT-La Plata, CONICET
Calles 47 y 115 (1900) La Plata, Argentina

[#]Corresponding author. lodeiro@biol.unlp.edu.ar

Running title: Regulation of lateral flagella in *B. diazoefficiens*

Key words: *Bradyrhizobium*, flagella, expression, *lafR*, *flbT*

ABSTRACT

Bradyrhizobium diazoefficiens, the soybean N_2-fixing symbiont, possesses a dual flagellar system comprising a constitutive subpolar flagellum and inducible lateral flagella. Here, we analyzed the genomic organization and biosynthetic regulation of the lateral-flagellar genes. We found that those genes are located in a single genomic cluster, organized in two monocistronic transcriptional units and three operons, one possibly containing an internal transcription start site. Among the monocistronic units is blr6846, homologous to the Class-IB master regulators of flagella synthesis in *Brucella melitensis* and *Ensifer meliloti*, and required for the expression of all the lateral-flagellar genes except *lafA2*, which locus encodes a single lateral flagellin. We therefore named blr6846 *lafR* (lateral-flagellar regulator). Despite its similarity to two-component response regulators and its possession of a phosphorylable Asp residue, *lafR* behaved as an orphan response regulator by not requiring phosphorylation at this site. Among the genes induced by *lafR* is $flbT_L$, a Class-III regulator. We observed different requirements for $FlbT_L$ in the synthesis of each flagellin subunit. While accumulation of *lafA1*, but not *lafA2*, transcripts required $FlbT_L$; the production of both flagellin polypeptides required $FlbT_L$. Moreover, the regulation cascade of this lateral-flagellar regulon appeared not as strictly ordered as those found in other bacterial species.

IMPORTANCE

Bacterial motility seems essential for the free-living style in the environment and therefore, these microorganisms allocate a great deal of their energetic resources to the biosynthesis and functioning of flagella. Despite energetic costs, some bacterial species possess dual flagellar systems, one of which is a primary system normally polar or subpolar, and the other is a secondary, lateral system that is produced only under special circumstances. *Bradyrhizobium diazoefficiens*, the N_2-fixing symbiont of soybean plants, possesses dual flagellar systems, among which the lateral system that contributes to swimming in wet soil and competition for nodulation, is expressed under high energy availability as well as under requirement for high torque by the flagella. Structural organization and transcriptional regulation of the 41 genes that comprise this secondary flagellar system seem adapted to adjust bacterial energy expenditures for motility to the soil's environmental dynamics.

INTRODUCTION

Flagella-driven swimming motility—a characteristic trait of many bacterial species—is essential for colonization of diverse niches in environments such as seas, freshwaters, sediments, soils, and the organs of plant or animal hosts. This form of bacterial locomotion requires the propulsion provided by flagella as well as a guidance system mediated by chemotaxis (1).

Flagella are complex organelles formed by three main structures: a basal body that anchors the flagellum to the cell envelope, a filament that projects out from the cell often with a length greater than the cell body itself, and a hook that connects the basal body to the filament (Fig. S1). The basal body, the most complex of these substructures, is responsible for two critical tasks: exporting the hook and filament proteins synthesized in the cytoplasm towards the extracellular space (2, 3) and providing the rotational motion of the flagella (4-6). For the first task, an export apparatus is embedded in the inner cell membrane ending in a rod that crosses the cell envelope and delivers the hook and filament polypeptides. Because the rod's internal channel is narrow, the polypeptides must pass through in a partially unfolded state, which conformation is stabilized by specific chaperones through proton-motive force and ATP hydrolysis as energy sources. For the second task, the basal body contains the flagellar motor, composed of a stator in the inner cell membrane and a rotor formed by a ring of several protein subunits that rotates inside the stator by proton- or sodium-ion–motive force. In turn, the hook and the filament are formed by the polymerization of thousands of monomers of structural proteins and are held together by specific hook-filament junctions (7, 8). The hook is a flexible connector that transmits motor rotation in the form of waves to the flagellar filament, which extension in turn rotates while undulating like an Archimedean screw to drag or thrust the cell in an aqueous medium, depending on whether the flagellum is ahead or behind the cell, respectively (9). In Gram-negative bacteria, the whole structure passes through the inner membrane, the peptidoglycan layer, and the outer membrane with each layer containing rings that behave like bushings. The more than 40 genes that encode the basal body, the hook, the filament, the rings, and the auxiliary and regulatory proteins lie in a limited number of operons that, together with the chemotaxis genes, comprise the flagellar regulon.

The synthesis and assemblage of the bacterial flagellum require a substantial organization in order to ensure that all the major structures are completed sequentially from the membrane-associated elements to the extracellular components (10, 11). Thus, depending on the species, the regulation of flagellum biosynthesis comprises three or four principal steps, which stages have been carefully studied in model systems such as *Caulobacter crescentus*, *Ensifer meliloti*, *Escherichia coli*, *Pseudomonas* spp., *Salmonella enterica*, and *Vibrio* spp., among others (12-14). In general, a master regulator (Class I) induces the expression of several flagellar operons (Class II) that encode the basal body, the hook and hook-related proteins, and a regulator of the synthesis of the filament monomers or flagellins. Therefore, those flagellins (Class III) are synthesized in the final step, with the basal body and the hook already in position. This strategy insures that no energy is wasted on flagellin synthesis and export before these proteins are required (10, 13).

The rotation of the flagellar motor defines whether a bacterium swims in a given direction or erratically. In general, when the flagella rotate in a single direction, the bacteria swim in linear runs; which stretches are interrupted when flagellar rotation switches direction or stops (15-18). The frequency at which these changes in direction occur are governed by the chemotaxis system in response to chemical stimuli (*i. e.*, attractant or repellent gradients) present in the medium (18). As with the flagellar genes, the chemotaxis loci are often arranged in operons under control by the same regulators that govern the synthesis of flagellins and therefore are also grouped in Class III of the flagellar regulon (13).

Bradyrhizobium diazoefficiens, the soybean N_2-fixing symbiont, is a soil α-proteobacterium that possesses two different flagellar systems with independent evolutionary origins (19, 20). One of those systems involves a subpolar flagellum closely related to the one in *C. crescentus*, while the other is characterized by lateral flagella similar to those in *E. meliloti*

(20). The expression of each flagellar system is also different. The subpolar system seems constitutive within a range of conditions; by contrast, the expression of the lateral system requires arabinose as a carbon source or viscosity in the culture medium or the presence of obstacles in the swimming path (20-22). Hence, growth in liquid medium with mannitol as the carbon source does not permit the expression of the lateral flagella. Transcriptomic studies have also indicated that conditions of microoxia (23) or iron deficiency (24) prevent the expression of lateral-flagellar genes, while permanent exposure to moderate oxidative stress induces those loci (25). In the example of *E. meliloti* and its close relative *B. melitensis*, flagellar expression is also under strict control by specific nutritional, physiological and population-size requirements (26-29).

In contrast to other species having dual flagellar systems that use one exclusively for swimming in a liquid medium and the other only for swarming on surfaces, both the flagellar systems of *B. diazoefficiens* may be utilized together in liquid medium and interact to produce an emergent swimming performance that allows the bacterium to continually swim along side solid surfaces (20). Only the subpolar system, however, responds to chemotactical stimuli, whereas only the lateral system contributes to swimming in viscous agar-containing medium (20). Although neither of these flagellar systems is required for the nodulation of soybean plants (30), bacterial motility might be essential for nodule occupation in competition against populations of compatible rhizobia in the soil (31). In earlier work, we obtained a derivative of *B. diazoefficiens* USDA 110 having higher motility by *in-vitro* selection (21). The inoculation of this derivative on experimental soybean crops planted in soils with dense soybean-nodulating competitor populations resulted in an enhanced nodule occupation by the derivative and promoted a higher soybean-grain yield (21, 31). Further studies indicated that the lateral-flagellar system of this derivative became derepressed upon culture in liquid medium with mannitol as the carbon and energy source (21, 22). Therefore, the control of lateral-flagellar synthesis in this species should take into account the cell's needs on the basis of the environmental conditions in order to coordinate the activity of both flagellar systems, which would appear to be essential for the symbiotic interaction with soybean plants. To better understand the regulation of these genetically controlled functions, in the study reported here, we investigated the organization and transcriptional control of the lateral-flagellar genes of *B. diazoefficiens* USDA 110.

RESULTS

Identification and characterization of lafR*, the master regulator of lateral-flagellar synthesis in* B. diazoefficiens *USDA 110*

In *E. meliloti* flagellar expression is controlled by a regulatory circuit composed of the LuxR-type master regulators VisNR and the OmpR-like transcriptional activator Rem (28). In a similar fashion, the LuxR-type VjbR and the OmpR-like FtcR are master regulators of flagellar expression in *B. melitensis* (32). Although the regulation circuit of neither VisNR nor VjbR is restricted to flagellar-gene expression, the Rem and FtcR regulators seem to be more specific (28, 32). In addition, since the expression of *rem* and *ftcR* is regulated by VisNR and VjbR, respectively; the LuxR-type components were classified as Class IA whereas the OmpR-like components were considered as Class IB (28, 32). Within the complete genomic sequence of *B. diazoefficiens* USDA 110 (33), we could not find homologs to *visNR* or *vjbR*, but the locus tag blr6846 (Ga0076376_112362 in the reannotation at the IMG database)—it located near the cluster of genes that encode the lateral flagella in *B. diazoefficiens*—encodes a predicted OmpR-like transcriptional-response regulator of 256 residues homologous to Rem and FtcR and harboring the typical receiver and helix-turn-helix DNA-binding domains (Fig. 2SA). The high similarity among these three OmpR-like transcriptional-response regulators, as well as the position of blr6846 with respect to the lateral flagellar-gene cluster led us to suspect that blr6846 might be a master regulator of the synthesis of the lateral flagella in *B. diazzoefficiens*. This suspicion was reinforced by the observation that the expression of blr6846 is dependent on the carbon source in a manner similar to that of the production of the lateral flagellins LafA1 and

Journal of Bacteriology

LafA2, since blr6846 is expressed in arabinose-grown cultures at substantially higher levels than in mannitol-containing cultures (Fig. 1A-B). In addition, a mutant harboring a Km-resistant cassette inserted at base 7,543,291, in the middle of the coding sequence of blr6846, thus disrupting the connection between the receiver and helix-turn-helix DNA-binding domains (Fig. 2SB), was found to lack lateral flagellins even when grown with arabinose as the carbon source (Fig. 1A). The production of the lateral flagellins was restored after introducing a wild-type copy of blr6846 in the pFAJ1708 replicative plasmid, indicating that the defective phenotype resulted from the disruption of the coding sequence of blr6846. In addition, the lateral-flagellin production was restored in the wild-type strain grown with mannitol when blr6846 was expressed constitutively from the replicative plasmid (Fig. 1A), demonstrating that the expression of blr6846 was sufficient to produce the lateral flagellins under this condition. However, the polypeptide levels of LafA relative to those of FliC were variable in the complemented strains among the different experiments. Since pFAJ1708 is stable in *B. diazoefficiens*, we have no explanation for the observed instability in LafA recovery, which nevertheless does not rule out the conclusions that the *lafR*::Km mutation may be complemented in *trans*, and that the presence of *lafR* in *trans* is sufficient for lateral flagellin synthesis in mannitol. The blr6846 mutant achieved a smaller swimming halo than the wild-type in soft agar, which area was similar to that produced by the lateral flagellin-deficient mutant Δ*lafA* (Fig. 1C). This defect in swimming, observed in the mutants within the WT USDA 110 background, was also displayed by a blr6846 mutant in the LP 3004 background (the USDA 110 Sm-resistant derivative) and by another blr6846 mutant in the LP 3008 background (the LP 3004-derivative with higher motility; not shown). In addition, motility of the *lafR*::Km mutant was restored by *trans* complementation with pFAJ::*lafR* (Fig. 1C), indicating that *lafR* expression was sufficient to produce functional lateral flagella. Taken together, these results corroborated that blr6846 might have similar roles to those of *rem* and *ftcR* so that hereafter we will refer to blr6846 as *lafR* for "lateral flagella regulator" and have accordingly renamed the Km-insertion mutation *lafR*::Km.

LafR as an orphan response regulator

A critical difference observed in the amino-acid sequence of LafR with respect to its counterparts Rem and FtcR is the presence of an Asp residue at position 50, susceptible to phosphorylation as in the typical transcriptional-response regulator OmpR (Fig. S2A). By contrast, Rem and FtcR possess a Glu at this position, the latter residue being larger than Asp by an additional methyl group (28, 32). Therefore Rem and FtcR may function as if they were continually activated (32), while LafR might require phosphorylation for activation; which property would be consistent with the inducible nature of lateral flagella in *B. diazoefficiens*. We could not find, however, any putative histidine kinase associated with *lafR*. In order to elucidate this question, we constructed the single-substitution mutants *lafR*D50A, *lafR*D50G, and *lafR*D50E (Table S1) in which the Asp50 residue was replaced by an Ala (without the carboxyl group of Asp), a Gly (without any residue) or a Glu (as in Rem and FtcR; *cf*. Fig S2A), respectively. Therefore, if phosphorylation of the Asp50 was required, neither *lafR*D50A nor *lafR*D50G would be activated, while *lafR*D50E would likely be constitutively active. Nevertheless, we observed the same profile of activation in all three mutants and in the wild-type—*i. e.*, the lateral flagellins were produced with arabinose but not with mannitol as the carbon source (Fig. 1D). Together, these results indicated that LafR behaves as an orphan response regulator whose activation seems not to require phosphorylation of Asp50 by a histidine-kinase sensor.

The function of lafR *cannot be replaced by* rem

To further characterize the possible similarity between *lafR* and *rem*, we looked for possible cross-complementation of these genes in the *B. diazoefficiens* and *E. meliloti* mutants.

Thus, we introduced a wild-type copy of *rem* carried by pFAJ1708 into the *B. diazoefficiens lafR* mutant and, reciprocally, introduced a wild-type copy of *lafR* into the *E. meliloti rem* mutant Rm2011mTn5STM.1.08.H02 (hereafter, Δ*rem*, Table S1). The flagellins, however, were not observed in the cross-complemented strains (Fig. 1E). Since the controls complemented with the transcriptional regulator of the same species did produce flagellins, we concluded that either LafR or Rem are not stably expressed in *E. meliloti* or *B. diazoefficiens*, respectively, or the failure of cross-complementation in the experimental strains may be owing to lack of recognition in the interaction between the heterologous proteins and DNAs.

Operon organization in the lateral-flagellar–gene cluster

The 41 lateral-flagellar genes of *B. diazoefficiens* are grouped in a single cluster, although evidence for the origin of that acquisition through horizontal gene transfer could not be found (20). In addition, the lack of chemotaxis genes in the vicinity of this cluster—in agreement with the lack of chemotactic response exerted by the lateral flagellar system (20)—suggests that this cluster might constitute the complete lateral-flagellar regulon. Through the use of different bioinformatic tools (*e. g.*, MicrobesOnline Database, ProOpDb, and DOOR[2]), we predicted the operon structure of the gene cluster that is schematized in Fig. 2A and found a new open-reading frame (ORF) between *fliR*$_L$ (bll6849) and *flgJ*$_L$ (bll6850), which sequence we named bll6849.5. According to this analysis, the lateral-flagellar–gene cluster might be divided into at least five putative operons and three monocistronic transcriptional units: *lafR*, *lafA1*, and *lafA2*. All transcriptional units are conserved in *E. meliloti* and *B. melitensis*, but the synteny contains some differences (Fig. S3). In a recent study, the genome-wide transcription-start-sites map of *B. diazoefficiens* USDA 110 grown in peptone–salts–yeast-extract–arabinose medium was established (34), indicating different operon structures for the lateral-flagellar region from those predicted by the bioinformatic analysis (Fig. 2A). To resolve this contradiction, we designed primers to amplify, by RT-PCR, eight intergenic regions that should differ in the resulting transcripts according to whether the distribution of polycistronic mRNAs from this genomic cluster under our conditions is as predicted by bioinformatics or as reported in the experimental transcription–start-site mapping (34). The regions chosen were: region 1 from 3'-*flgJ*$_L$ (bll6849) to 5'-*fliR*$_L$ (bll6850; further encompassing the intergenic regions upstream and downstream from bll6849.5), region 2 from 3'-*flgE*$_L$ (bll6858) to 5'-bll6859, region 3 from 3'-*fliK*$_L$ (bll6860) to 5'-*motC* (bll6861), region 4 from 3'-*fliF*$_L$ (bll6864) to 5'-*lafA2* (bll6865), region 5 from 3'-*lafA2* (bll6865) to 5'-*lafA1*(bll6866), region 6 from 3'-*lafA1* (bll6866) to 5'-*fliP*$_L$ (bll6867), region 7 from 3'-*flgB*$_L$ (bll6876) to 5'-*flhB*$_L$ (bll6877), and region 8 from 3'-*fliN*$_L$ (bll6879) to 5'-bll6880 (Fig. 2A-C). By this approach, we would be able to detect amplification only where the mRNA is polycistronic for the adjacent genes probed (35). We observed that no amplification occurred only between 3'-*fliF*$_L$ and 5'-*lafA2*, and between 3'-*lafA2* and 5'-*lafA1* (Fig. S4), suggesting the existence of two operons encompassing bll6847-*fliF*$_L$ (Operon I) and *lafA1-motA* (Operon II), with *lafA2* remaining as a monocistronic transcriptional unit situated between those two operons. In addition, *lafR* and *flgF1*$_L$-*fliI*$_L$ (Operon III) can be considered different transcriptional units since they are encoded in the opposite strand (Fig. 2A).

LafR activation of three of the four transcriptional units

We analyzed the requirements for LafR with respect to the transcriptional profile of the lateral flagellar regulon by quantitative retrotranscribed PCR (qRT-PCR) with whole RNA from the wild-type and the *lafR*::Km mutant. We chose as representative genes of each transcriptional unit: *fliF*$_L$, *motC*, *flbT*$_L$, and *flgN*$_L$ for Operon I; *fliM*$_L$, *fliG*$_L$, *fliL*$_L$, *fliP*$_L$, and *lafA1* for Operon II; and *flgF1*$_L$ and *fliI*$_L$ for Operon III along with both the monocistronic transcriptional units *lafR* and *lafA2* (Fig. 2A) for amplification. Fig. 3A summarizes the results of the qRT-PCR assays. According to the relative expression levels obtained with the *lafR*::Km mutant in comparison to the wild-type, we observed that *lafR* was not autoregulated; but with respect to the Operons I-III, *lafR* was a positive regulator, in agreement with the previous observation that the *lafR*::Km mutant was unable to produce lateral flagellins (Fig. 1). In contrast, the mutation of *lafR* did not produce substantial changes in the abundance of the *lafA2* transcript.

To search for possible common motifs in the the 5' untranslated regions (5' UTRs) of the three operons, we performed sequence comparisons with the MEME Suite (36). A *de-novo* search for these sequences located a possible common motif shared by the LafR-induced operons (Fig. 2B). The motif is located approximately at the same distance from the transcription–start-site base pair (+1) of each operon. Of relevance here is that a search with the MAST algorithm at the MEME server did not locate this motif either upstream from the *E. meliloti rem* sequence—in agreement with the lack of cross-complementation between *lafR* and *rem*—or upstream from any other *B. diazoefficiens* gene, suggesting that this motif might be shared by the *lafR*-dependent promoters.

The lack of changes in *lafA2* transcript accumulation between the wild-type and the *lafR*::Km mutant indicates that another regulation is likely to be responsible for the inhibition of LafA2-polypeptide production in this mutant. We suspected that this role might be fulfilled by FlbT, which protein is known as a translational regulator of flagellin synthesis in other bacteria (37, 38).

FlbT$_L$ as a positive regulator of flagellin synthesis

To investigate whether or not FlbT$_L$ regulates flagellin synthesis in *B. diazoefficiens* as in other bacteria, we constructed a deletion mutant in *flbT$_L$* by eliminating 195 bp from the middle of the coding region, (between bases 7,549,514 and 7,549,709) without any alteration in the reading frame (Fig S5). This mutant (Δ*flbT$_L$*) would thus be expected to produce an internally deleted gene product without any polar effects on genes downstream in the operon. We observed that Δ*flbT$_L$* (LafR$^+$/FlbT$_L^-$) was unable to produce LafA1 and LafA2 with arabinose as the carbon source and that this phenotype was reversed when Δ*flbT$_L$* was complemented in *trans* with a wild-type copy of *flbT$_L$* carried in the replicative plasmid pFAJ::*flbT$_L$* (Fig. 4A). Likewise, the

$\Delta flbT_L$-mutant swimming motility in soft agar was compromised, similar to the analogous defect in the Δ*lafA* and *lafR*::Km mutants, and this phenotype was partially complemented in *trans* (Fig. 1C). These results indicated that, as in *B. melitensis* (38), $FlbT_L$ is required for lateral flagellin synthesis.

Next, we extended the analysis of the transcriptional profile of the lateral-flagellar operons by incorporating an $LafR^{-}/FlbT_L^{C}$ strain (*lafR*::Km mutant complemented with $flbT_L$ in *trans* under the control of a constitutive promoter). Using the same approach as before (Fig. 3A), we compared the relative expression of *motC*, $fliF_L$ (Operon I), $fliM_L$, $fliL_L$, *lafA1*(Operon II), and *lafA2* in the wild-type to both the $LafR^{+}/FlbT_L^{-}$ and the $LafR^{-}/FlbT_L^{C}$ genetic backgrounds. We observed that the deletion of $flbT_L$ had no effect on the expression of any of the genes tested, except for *lafA1*: in this gene, however, transcript accumulation was inhibited when $flbT_L$ bore a similar mutation to that of *lafR* (Fig. 3B). Because $flbT_L$ was itself induced by *lafR*, the observed effect of the *lafR* mutation on *lafA1* expression could be indirect as a result of a downregulation of $flbT_L$ within the *lafR*::Km genetic background. Therefore, we evaluated the expression of *lafA1* in the $LafR^{-}/FlbT_L^{C}$ genetic background and observed that transcript accumulation of *lafA1* was partially restored, although the relative expression of *lafA1* in the wild-type with respect to that of the mutant was still significant, indicating that $flbT_L$ had a partial influence on the control of *lafA1*-transcript accumulation. Conversely, the adjacent gene $fliL_L$ within the same operon responded only to *lafR* since that locus was downregulated within the $LafR^{-}/FlbT_L^{C}$ genetic background (similar to the result with the *lafR*::Km mutant) but was not affected in the $LafR^{+}/FlbT_L^{-}$ background (Fig. 3B).

Although a transcript start site of *lafA1* could not be detected by RNA-sequencing analysis (34), the pattern of differential regulation on the part of *lafA1* with respect to the rest of Operon II prompted us to investigate whether an internal promoter activity might be found within Operon II upstream from *lafA1*. To this end, we cloned the DNA segments between the 3' end of $fliP_L$ and the ATG of *lafA1* (P*lafA1*) and between the 3' end of *lafA1* and the ATG of *lafA2* (P*lafA2*) in the replicative plasmid pCB303 upstream from the promoterless *lacZ* site and measured the resultant β-galactosidase activity of the fusions. We observed more than twice the activity in the pCB::P*lafA1* plasmid carrying the P*lafA1*::*lacZ* fusion than in pCB::P*lafA2* plasmid carrying the P*lafA2*::*lacZ* fusion, without differences among the wild-type, *lafR*::Km, or $\Delta flbT_L$ genetic backgrounds (Fig. 5); thus indicating the existence of an active promoter upstream from *lafA1*, which locus—as with *lafA2*—would not be under transcriptional control of LafR or $\mathrm{FlbT_L}$. To further investigate the difference in the responses of *lafA1* and *lafA2* to $\mathrm{FlbT_L}$, we compared the nucleotide sequences and RNA predicted structures of the 5' UTRs of these transcripts. To this end, we used the sequence within the *lafA2* 5' UTR beginning at the experimentally identified transcription start site at 118 nucleotides upstream from the ATG initiation codon (34) and extending through the first 17 codons of the coding sequence (39) in comparison with a putative 5' UTR of *lafA1* starting also at 118 nucleotides upstream from the ATG and continuing through the first 17 codons of the coding sequence. Despite the high conservation among these sequences, we observed a gap near a sequence complementary to the ribosome binding site (RBS) in *lafA2* (Fig. S6A). In four of seven predicted stable secondary structures of the *lafA1* 5'-UTR region, a small loop arose at the RBS complementary sequence, which conformation might loosen RBS occlusion, but would leave the ATG initiation codon in a double-helix stretch (Fig. S6B). By contrast, the other three structures as well as the two predicted stable secondary structures of the *lafA2* 5' UTR had the RBS site in a double-helix stretch, but the ATG start codon was predicted in a single-strand region (Fig S6B-C). Taken together, these results are consistent with the postulated presence of a constitutive internal active promoter in Operon II for *lafA1* transcription. The most plausible assumption to explain the above results may be that *lafA1* mRNA stability might be controlled by $\mathrm{FlbT_L}$ differently from that of *lafA2* (Fig. 2A).

Despite *lafA1*- and *lafA2*-transcript production, lateral flagellins were observed in neither *B. diazoefficiens* USDA 110 carrying pFAJ::$flbT_L$ cultured with mannitol nor the *lafR*::Km mutant carrying pFAJ::*flbT*$_L$ cultured with arabinose (Fig. 4A). We reasoned that these observations might be owing to the lack of a filament-export apparatus under conditions where LafR is not produced, thus leading to an accumulation of LafA1 and LafA2 inside the cell. To test for this possibility, we obtained total cellular proteins and performed a Western blot with an LafA-specific polyclonal antibody (22). As expected, the wild-type *B. diazoefficiens* cultured with mannitol did not accumulate LafA intracellularly, whereas the same strain cultured with arabinose contained a clearly visible band of binding by the anti-LafA antibody in the Western blot at the expected molecular mass. In contrast, complementation of the wild-type cells with *flbT*$_L$ in *trans* failed to restore LafA accumulation in either the wild-type cells grown with mannitol or the *lafR*::Km mutant grown with arabinose, where *lafR*, was not expressed (Fig 4B).

DISCUSSION

The lateral-flagellar genes of *B. diazoefficiens* lie in a single cluster encompassing 34,823 bp, organized in two monocistronic transcriptional units and three operons, with one of those three possibly having an independent internal promoter. In addition, no chemotaxis genes are present in this cluster. The expression of the three operons required the protein product of *lafR*, which gene constitutes one of the monocistronic transcriptional units identified. The regulation of LafR, together with the protein's sequence homology to known Class-IB master regulators, suggests that LafR is the Class-IB master regulator of lateral-flagella synthesis in *B. diazoefficiens*. In α-proteobacteria there are different types of master regulators, including two-component systems such as the *ctrA-cckA* of *Rhodobacter capsulatus* (40), or OmpR-like transcriptional activators such as the *rem* of *E. meliloti* (28) or the *ftcR* of *B. melitensis* (32). These latter activators, in turn, are controlled by the respective LuxR-type systems, *visNR* and *vjbR* (32, 41, 42), which respond to cell-cycle cues or environmental stimuli indicating the need to activate or inactivate flagellar synthesis. In the particular example of *B. diazoefficiens*, respiration rate might be just such a signal linked to the transcription of the lateral-flagellar regulon. Previous reports indicated that situations diminishing the respiration rate, such as microaerobiosis, the bacteroid state (23) or iron deficiency (24), downregulate the lateral-flagellar–regulon transcription; while situations known to increase the oxygen consumption, such as permanent exposure to moderate oxidative stress (25) or the use of arabinose as the sole carbon source (43, Cogo *et al.*, unplublished data), promote that transcription. Moreover, these changes in transcription were not observed in the subpolar-flagellar regulon, indicating that those stimuli act specifically on the lateral flagella. Although we could not find *visNR* or *vjbR* homologs in *B. diazoefficiens*, the RegSR two-component system—it regulating the responses to microoxia—was reported to modify the expression specifically of *lafR* and the lateral-flagellar regulon after a switch from oxic to microoxic (O_2 concentration <0.5%) conditions (44). In agreement with these results, a TetR-family transcriptional regulator was also found to repress the lateral-flagellar genes in a coordinated manner along with genes encoding high-affinity cytochromes and oxidative-stress detoxification products, without affecting the subpolar-flagellar genes (45). Therefore, several stimuli related to the energy status of the cell are able to trigger lateral-flagellar expression in *B. diazoefficiens* without affecting subpolar-flagellar expression. Such stimuli seem transmitted to the Class-IB regulator *lafR* by different Class-IA regulators from those of *E. meliloti* or *B. melitensis*. In turn, *lafR* itself could be part of a two-component system, but two observations argue against this possibility. First, a putative histidine kinase could not be found for this system; second, the phosphorylable Asp50 residue of LafR may be replaced by Ala, Gly or Glu without alterations in the response of flagellin synthesis to the carbon source present in the culture medium, indicating that Asp50 is not phosphorylated in LafR.

The correlation between operon organization and flagellar substructures shown in Fig. S1 indicates that all the genes induced by LafR are among the Class-II genes transcribed in the second step of the cascade, although the strict temporal order observed in other species (11) is not reflected by the distribution of the flagellar genes among the three operons. Most of the flagellar motor (4) is encoded in Operon II, except the MS ring component FliF$_{L}$ and the stator protein MotB, both of which loci are encoded in Operon I. Moreover, the genes encoding the export apparatus (2, 3), which component is also part of the basal body, are scattered among the three operons. The export of the hook and filament proteins from the cytoplasm to the extracellular space through the narrow space inside the rod may require: (i) their recruitment at the export gate that is formed by FlhA$_{L}$, FliQ$_{L}$, FliR$_{L}$ (Operon I), FlhB$_{L}$, and FliP$_{L}$ (Operon II); (ii) ATP hydrolysis catalyzed by FliI$_{L}$ (Operon III); (iii) the chaperon activities of FlgN$_{L}$ (Operon I) and FlgA$_{L}$ (Operon II); and (iv) the control switch in the export sequence between hook and filament effected by FliK$_{L}$ (Operon I). The structure of the rod apparatus and the rings that act as bushings in the membranes and the peptidoglycan layer are mostly encoded in Operon II, except for *flgF$_{L}$*, which locus is in Operon III. The gene *flgJ$_{L}$* that encodes the β-N-acetylglucosaminidase required for the hydrolysis of the peptidoglycan layer in order to allow passage of the P-ring and the rod (46), however, is in Operon I (Fig. S1). Therefore, a functional export apparatus in this flagellar system requires the expression of genes from the three operons. Some genes are also missing—such as *fliD* encoding the filament cap and the *fliI*-associated *fliH* and *fliJ*—which loci might be encoded in the hypothetical open-reading frames that we could not yet identify. In addition, a complementation by proteins from the subpolar-flagellar system cannot be discarded, although this possibility seems unlikely in view of the substantial difference in structure and function between the two flagellar systems.

Moreover, Operon I encodes FlbT$_{L}$, a regulator whose homologs in *C. crescentus* and *B. melitensis* regulate the expression of Class-III genes (37, 38). Despite that homology, however, FlbT plays opposite roles in those systems: Whereas in *C. crescentus* FlbT is an inhibitor of the translation of flagellin transcripts, in *B. melitensis* that protein is required for translation. The target site of FlbT-dependent regulation—it reported to lie within the 5' UTR of the mRNA—regulates translation and mRNA stability, but the existence of an as-yet-unknown intermediate for the formation of the FlbT–5'-UTR-mRNA complex might explain these opposite actions

(39). Moreover, some effect of FlbT on the activity of the flagellin-gene promoter has also been detected (38, 47). In the example of the *B. diazoefficiens* lateral flagella, the role of $\mathrm{FlbT_L}$ in *lafA1* and *lafA2* expression was even more intriguing. As in *B. melitensis*, $\mathrm{FlbT_L}$ was required for lateral-flagellin production (Fig. 4), including LafA1 and LafA2 in the low-molecular-mass band (20); but, as a striking exception to the known flagellar systems, the flagellin gene *lafA1* lies at the 3’ end of Operon II under transcriptional control of the Class-IB regulator LafR, instead of being a Class-III gene encoded in a monocistronic transcriptional unit. After an evaluation of the effects of LafR and $\mathrm{FlbT_L}$ on $fliL_L$- and *lafA1*-transcript accumulation (Fig. 3B), LafR activity proved to be only in part required for *lafA1* expression, which result is consistent with the existence of an internal promoter within Operon II upstream from *lafA1*. The activity of this internal promoter would not be regulated by LafR or $\mathrm{FlbT_L}$, but the differences in nucleotide sequence and predicted secondary structure between the 5’ UTRs of *lafA1* and *lafA2*, as well as the discrepancies in the responses of these genes to $\mathrm{FlbT_L}$ with respect to transcript abundance suggest that the *lafA1* transcript would be more unstable than the *lafA2* transcript in the absence of $\mathrm{FlbT_L}$. Therefore, both the expression and the subsequent mRNA stability of *lafA1* seem to be under a mixture of Class-IB and Class-III regulation; whereas the *lafA2* monocistronic transcript would require neither LafR nor $\mathrm{FlbT_L}$ for accumulation, and in this instance the role of $\mathrm{FlbT_L}$ might be restricted to some form of translational control. Neither LafA1 nor LafA2 seemed to accumulate in the cytoplasm of cells expressing $flbT_L$ from a multicopy plasmid when the export apparatus was not formed, indicating that an additional system coordinates LafA production and secretion. We identified $flaF_L$ as being located immediately upstream from $flbT_L$ in Operon I. In *C. crescentus* and *B. melitensis* FlaF was described as a counterregulator of FlbT through an as-yet-unknown mechanism (38, 47). If $\mathrm{FlaF_L}$ has a similar role in *B. diazoefficiens*, that protein might prevent FlbT-dependent translation of the *lafA2* and *lafA1* transcripts until the export apparatus becomes functional. Fig. 6 presents the scheme of the regulatory circuit that may be deduced from our results.

The present results indicate that the hierarchies of regulation at the level of transcription are not as strict as in model systems, but instead seem more similar to the regulation in *B. melitensis*, where the flagella are synthesized during a short period in the bacterial culture (38). This lack of a hierarchy might constitute an adaptation to the use of these flagella only when required by the environmental conditions. In the example of the lateral flagella of *B. diazoefficiens*, the environmental conditions seem to be related either to energy availability and demand—in particular the availability of oxygen (23) and the carbon source (this work)—or to a requirement for higher torque by the flagella, such as upon an alteration in the viscosity and/or the porosity of the medium (20). A monitoring of these situations might be essential in order for this bacterium to adapt its energy expenditures for motility to the soil's environmental dynamics.

MATERIALS AND METHODS

Bacterial strains and culture conditions

Table S1 summarizes the bacterial strains and plasmids used in this work. *Bradyrhizobium diazoefficiens* was grown in HM salts (48) plus 0.1% yeast-extract (HMY) with 0.5% mannitol or 0.5% arabinose as the carbon source. Total biomass was estimated by the measurement of the optical density at 500 nm (OD_{500}) and the number of viable bacteria by the number of colony-forming units (CFUs) on yeast extract-mannitol (49) agar plates (YMA). For swimming-motility analysis, bacteria were inoculated with a sterile toothpick on semisolid AG medium (48) containing 0.3% (w/v) agar and the motility halo registered as described (21). For conjugation, a modified peptone salt–yeast-extract medium (50) was employed. *Escherichia coli* was grown in Luria-Bertani medium (51). Antibiotics were added to the media at the following concentrations ($\mu g.ml^{-1}$): streptomycin (Sm), 400 (*B. diazoefficiens*) or 100 (*E. coli*); spectinomycin (Sp), 200 (*B. diazoefficiens*) or 100 (*E. coli*); kanamycin (Km), 150 (*B. diazoefficiens*) or 25 (*E. coli*); ampicillin (Ap), 200; gentamicin (Gm), 100 (*B. diazoefficiens*) or

10 (*E. coli*); chloramphenicol (Cm), 20 (*B. diazoefficiens*); and tetracycline (Tc), 20 or 50 (*B. diazoefficiens* in liquid or solid cultures) or 10 (*E. coli*).

Bioinformatic methods

The multiple alignments were performed by means of CLUSTAL OMEGA (52) at the EMBL on-line server (53). The operon prediction was run in different online servers: The ProOpDB online server (54), the DOOR^2 on-line server (55), and the MicrobesOnline server tools (56). The analysis of these results in comparison with the transcription-start-sites map of *B. diazoefficiens* (34) was carried out with the Integrated Genome Browser (57). All the oligonucleotides were designed with Primer Blast (58). The RNA-secondary-structure prediction was carried out with Mfold 2.3 at 30°C with the other parameters as default (59). To find the common motif in the upstream DNA sequences of Operons I, II, and III, the MEME Suit was used (36). The scheme of the motif was built with the WebLogo server (60).

Genetic techniques and DNA manipulation

The cloning procedures—comprising DNA isolation, restriction digestion, ligation, and bacterial transformation—were performed as previously described (51). Bi- or triparental matings were performed with the *E. coli* DH5α or S17-1 strains, respectively, as had been previously described (61). Electroporation was performed with a Gene Pulser (Bio-Rad, Hercules, CA) at 1.5 V, 25 μF, and 200 Ω in a 0.1-cm–gap-width electroporation cuvette.

Oligonucleotide primers (Table S1) were purchased from Life Technologies (Buenos Aires, Argentina). DNA amplification was performed by the polymerase-chain reaction (PCR) in a Bioer Life Express thermocycler (Hangzhou, China) with the Taq DNA polymerase (Life Technologies, Buenos Aires, Argentina) for routine PCR or with the KAPA HiFi hot start (HS) DNA polymerase (Kapabiosystems, Woburn, MA) for the amplification of targets longer than 1,000 bp. The DNA sequencing was performed at Macrogen Corp. (Seoul, Korea).

To construct the *B. diazoefficiens lafR*::Km mutant, specific primers for blr6846 were designed. The fragment between the bp 7,542,881 and 7,543,632 was amplified from the *B. diazoefficiens* USDA 110 genomic DNA and cloned into the plasmid pG18mob2 (62) by means of an internal *Eco*RI site (at 7,542,999 bp) and a *Hind*III site generated from the LafR_Rv primer to generate the plasmid pG::*lafR*. Next, the Km cassette form the plasmid pUC4K (63) was cloned in an internal *Bam*HI site (7,543,291 bp) of the *lafR* fragment to give the plamid pG::*lafR*::Km The gene insertion of the Km cassette was performed by introducing the pG::*lafR*::Km into the wild-type strain *B. diazoefficiens* USDA 110 by biparental mating, with recombinant selection by growth on Km/Cm YMA, with subsequent screening for Km resistance and Gm sensitivity in order to select for the double-crossover mutant. The resulting strain was designated *lafR*::Km; this strain carries the Km-cassette insertion at the 7,543,291 position of the genomic DNA, thus disrupting the connection between the receiver and helix-turn-helix domains of *lafR* (*cf*. Fig. S2B).

The point mutations in the residue susceptible to phosphorylation (Asp50, Fig. S2A) were performed as described (51). The procedure stated in brief: PCR primers were designed complementary to the region spanning the mutation site of plasmid pG::*lafR*,—that plasmid DNA being the template for the reaction—but with single complementary base changes for one residue in both strands of the site in order to generate the desired point mutation. The PCR under the direction of those primers then amplified with Pfu DNA polymerase (Thermo Fisher Scientific, Waltham, MA) the entire plasmid including the mutation introduced in the primers to give the double-stranded DNA for the new mutant plasmid. The PCR mix was then treated with *Dpn*I and the template degraded. The reaction mix was desalted and transformed into *E. coli* DH5α. Because the position of the point mutation coincides with a *Sal*I restriction site in the wild-type sequence, we screened the clones by looking for resistance to digestion with this endonuclease. The positive clones were then corroborated by DNA sequencing. Those fragments with the point mutation were subcloned in the plasmid vector pK18*mobsacB* (64) to give the derivatives pK*sacB*::*lafR*D50A, pK*sacB*::*lafR*D50G, and pK*sacB*::*lafR*D50E. Each plasmid was transferred by mating to the wild-type strain, and simple crossovers were selected by Km resistance. Resolution of the plasmid was forced by plating the Km-resistant colonies in YMA supplemented with 10% (w/v) sucrose. The resulting clones were corroborated by PCR amplification and *Sal*I digestion of the fragment.

To construct the *B. diazoefficiens* Δ*flbT*$_L$ mutant, the crossover PCR method described by Link *et al*. (65) was applied to generate an in-frame deletion of the coding sequence of bll6854 (*flbT*$_L$). To this end, specific primers (FlbTUP_Fw and FlbTUP_Rv for PCR 1 and FlbTDW_Fw and FlbTDW_Rv for PCR 2) were designed for the amplification of upstream (118 bp) and downstream (99 bp) fragments of *flbT*$_L$ (PCR 1 and PCR 2 according to the methods in the references cited). Next, a PCR 3 reaction was run with primers FlbTUP_Fw and FlbTDW_Rv with an equal mixture of PCR 1 and PCR 2 products as template. The product of this PCR contains the 5´ and 3´ portions of *flbT*$_L$ interrupted by a short synthetic sequence (21 bp) that replaces an internal 195-bp fragment of the 411-bp coding sequence of *flbT*$_L$ without affecting the reading frame (*cf*. Fig S5). This construct was cloned into the pK18*mobsacB* vector to give the plasmid pK*sacB*::*flbT*$_L$. This plasmid was transferred to the wild-type strain by biparental mating and a resulting single crossover selected by Km resistance. Those simple recombinants were selected for further double crossovers by plating the bacteria in YMA supplemented with 10% (w/v) sucrose; thereafter, the resulting clones were subjected to PCR to distinguish the wild-type resolution of the plasmid from the mutant genotype. The correct in-frame deletion was verified by DNA sequencing.

Complementation experiments were performed by integrating the complete sequences of *lafR* or *flbT*$_L$ (amplified with primers LafRextFw/LafRextRv or FlbTextFw/FlbTextRv, respectively) into a replicative vector. Stated in brief, the 1,009-bp *lafR* and the 592-bp *flbT*$_L$ target sequences were amplified from *B. diazoefficiens* USDA 110 chromosomal DNA and then cloned into the *Xba*I/*Kpn*I sites of plasmid pFAJ1708 to create pFAJ::*lafR* and pFAJ::*flbT*$_L$, respectively. The recombinant plasmids were cloned with the *lafR* or *flbT*$_L$ genes under the direction of the strong, constitutive *nptII* promoter (66). These constructions were all confirmed by sequencing. Finally, each plasmid harboring the complete *lafR* or *flbT*$_L$ gene was transferred into the desired *B. diazoefficiens* strain by biparental mating, selected by Tc-resistance, and confirmed by PCR amplification and DNA sequencing.

To construct the *lacZ* fusions, the *lafA1* and *lafA2* promoter regions were amplified with the primers promA1_Fw and Rv and promA2_Fw and Rv, respectively (Table S1). The amplicons were digested with *Xba*I/*Pst*I, then cloned into the same restriction sites of the promoterless plasmid vector pCB303 carrying the complete sequence of the β-galactosidase gene (67). These constructions were named pCB::P*lafA1* and pCB::P*lafA2*, respectively. Each plasmid was transferred into the *B. diazoefficiens* USDA 110 strain by biparental mating, selected by Tc-resistance, and confirmed by PCR amplification. β-Galactosidase activity was measured as described (51).

RNA extraction and retrotranscribed PCR (RT-PCR)

Thirteen ml of *B. diazoefficiens* USDA 110 cells were harvested from liquid cultures, washed twice with 1 M NaCl, and disrupted with lysozyme in buffer TE, pH = 8.0 (30 min, 37°C). Total RNA was extracted through the use of TRIzol™ (Life Technologies, Buenos Aires, Argentina), following the manufacturers instructions, and the quality and quantity of the extract determined with a NanoDrop spectrophotometer (NanoDrop Technologies, Wilmington, DE). Aliquots (0.125 µg) were treated with DNase I (30 min, 37°C) and the cDNA synthesized with M-MLV reverse transcriptase (Life Technologies, Buenos Aires, Argentina) under the direction of random hexamer primers, following the manufacturers instructions. To check the quality of the cDNA preparation, PCR reactions were performed with the primers *phaR*_Fw and *phaR*_Rv and *relA*_Fw and *relA*_Rv (Table S1) as described previously (61). The absence of contaminating DNA was demonstrated by the lack of PCR amplification in an RNA sample that was not subjected to reverse transcription. Primers for the housekeeping gene *sigA* were used as a positive control (68).

To determine the operon structure, three RT-PCR reactions were performed with the appropriate cDNAs for each fragment (*cf*. Fig. 2B-D): two of the reactions amplified fragments of the coding sequence of each contiguous gene (positive control), while the third amplified a fragment encompassing the intergenic region between the target genes (35).

Quantitative real-time RT-PCR (qRT-PCR)

Amplification of the cDNAs obtained as described above was performed with the primers indicated in the Table S1 for each gene in a Line-Gene instrument (Bioer, Hangzhou, China) and analyzed with Line-Gene K Fluorescence Quantitative Detection System (Version 4.0.00 software). The ready-to-use iQ SYBR Green Supermix (BioRad, Hercules, CA) was used for all the reactions, according to the manufacturers instructions. Normalized expression values were calculated based on the absolute quantities of the gene of interest relative to the value for *sigA* (68).

Flagellin separation and analysis

The preparation of flagellins was carried out as described (30). Stated in brief, rhizobia grown in liquid medium to an OD_{500} = 1.0 were vortexed for 5 min and centrifuged at 10,000 × *g* for 30 min at 4°C. The supernatant was collected and incubated with 1.3% (v/v) polyethylene glycol (6000) and 166 mM NaCl for 2 h at 4°C. This suspension was centrifuged at 11,000 × *g* for 40 min at 4°C and the pellet resuspended in phosphate-buffered saline. For analysis, the samples were boiled in Laemmli loading buffer for 10 min and then separated by sodium-dodecyl-sulfate–polyacrylamide-gel electrophoresis (SDS-PAGE [69]). Polypeptide bands were revealed with Coomassie brilliant blue R250.

Total-proteins were prepared after lysis by boiling. The cell pellet was washed with 1 M NaCl solution, resuspended in Laemmli loading buffer, and heated for 10 min at 100°C. The samples were then centrifuged at 14,000 × *g* for 10 min and analyzed by SDS-PAGE. After electrophoresis, the gels were stained with Coomassie brilliant blue R250. Western blots were performed with specific anti-LafA polyclonal antibodies on the total proteins extracted from the cell pellets, as previously described (22, 70).

Acknowledgements

The authors are grateful to Dr. Donald Haggerty for English revision, and Dr. Anke Becker (Marburg University, Germany) for kindly providing the *E. meiloti* strains. This work was supported by Agencia Nacional de Promoción de la Investigación Científica y Tecnológica (ANPCyT) and Consejo Nacional de Investigaciones Científicas y Técnicas (CONICET), both from Argentina. EJM, JIQ, MJA, and ARL are members of the Scientific Career of CONICET. CD is a fellow of CONICET. The funders had no role in study design or data collection and interpretation. The authors declare that they have no conflict of interests.

References

1. Yuan J, Branch RW, Hosu BG, Berg HC. 2012. Adaptation at the output of the chemotaxis signalling pathway. *Nature* **484**: 233-236.

2. Evans LD, Hughes C, Fraser GM. 2014. Building a flagellum outside the bacterial cell. *Trends Microbiol* **22**: 566-572.

3. Minamino T. 2014. Protein export through the bacterial flagellar type III export pathway. *Biochim Biophys Acta* **1843**: 1642-1648.

4. Minamino T, Imada K. 2015. The bacterial flagellar motor and its structural diversity. *Trends Microbiol* **23**: 267-274.

5. Takekawa N, Nishiyama M, Kaneseki T, Kanai T, Atomi H, Kojima S, Homma M. 2015. Sodium-driven energy conversion for flagellar rotation of the earliest divergent hyperthermophilic bacterium. *Sci Rep* **5**: 12711.

6. Berg HC. 2016. The flagellar motor adapts, optimizing bacterial behavior. *Prot Sci* (in press). DOI: 10.1002/pro.305.

7. Fujii T, Kato T, Namba K. 2009. Specific arrangement of alpha-helical coiled coils in the core domain of the bacterial flagellar hook for the universal joint function. *Structure* **17**: 1485-1493.

8. Calladine CR, Luisi BF, Pratap JV. 2013. A "mechanistic" explanation of the multiple helical forms adopted by bacterial flagellar filaments. *J Mol Biol* **425**: 914-928.

9. Magariyama Y, Ichiba M, Nakata K, Baba K, Ohtani T, Kudo S, Goto T. 2005. Difference in bacterial motion between forward and backward swimming caused by the wall effect. *Biophys J* **88**: 3648-3658.

10. McCarter LL. 2006. Regulation of flagella. *Curr Opin Microbiol* **9**: 180-186.

11. Altegoer F, BangeG. 2015. Undiscovered regions on the molecular landscape of flagellar assembly. *Curr Opin Microbiol* **28**: 98-105.

12. Aldridge P, Hughes KT. 2002. Regulation of flagellar assembly. *Curr Opin Microbiol* **5**: 160-165.

13. Brown J, Faulds-Pain A, Aldridge P. 2009. The coordination of flagellar gene expression and the flagellar assembly pathway. In *Pili and Flagella, Current Research and Future Trends.* Jarrel, K.F. (ed). Trowbridge, Wiltshire. UK: Caister Academic Press, pp. 99-120.

14. Smith TG, Hoover TR. 2009.Deciphering bacterial flagellar gene regulatory networks in the genomic era. *Adv Appl Microbiol* **67**: 257-295.

15. Gotz R, Schmitt R. 1987. *Rhizobium meliloti* swims by unidirectional, intermittent rotation of right-handed flagellar helices. *J Bacteriol* **169**: 3146-3150.

16. Scharf B. (2002) Real-time imaging of fluorescent flagellar filaments of *Rhizobium lupini* H13-3: flagellar rotation and pH-induced polymorphic transitions. *J Bacteriol* **184**: 5979-5986.

17. Wei Y, Wang X, Liu J, Nememan I, Singh AH, Weiss H, Levin BR. 2011. The population dynamics of bacteria in physically structured habitats and the adaptive virtue of random motility. *Proc Natl Acad Sci U S A* **108**: 4047-4052.

18. Sourjik V, Wingreen NS. 2012.Responding to chemical gradients: bacterial chemotaxis. *Curr Opin Cell Biol* **24**: 262-268.

19. Liu R, Ochman H. 2007. Origins of flagellar gene operons and secondary flagellar systems. *J Bacteriol* **189**: 7098-7104.

20. Quelas JI, Althabegoiti MJ, Jimenez-Sanchez C, Melgarejo AA, Marconi VI, Mongiardini EJ, Trejo SA, Mengucci F, Ortega-Calvo JJ, Lodeiro AR. 2016. Swimming performance of *Bradyrhizobium diazoefficiens* is an emergent property of its two flagellar systems. *Sci Rep* **6**: 23841.

21. Althabegoiti MJ, López-García SL, Piccinetti C, Mongiardini EJ, Pérez-Giménez J, Quelas JI, Perticari A, Lodeiro AR. 2008. Strain selection for improvement of *Bradyrhizobium japonicum* competitiveness for nodulation of soybean. *FEMS Microbiol Lett* **282**: 115-123.

22. Covelli JM, Althabegoiti MJ, López MF, Lodeiro AR. 2013. Swarming motility in *Bradyrhizobium japonicum*. *Res Microbiol* **164**: 136-144.

23. Pessi G, Ahrens CH, Rehrauer H, Lindemann A, Hauser F, Fischer HM, Hennecke H. 2007. Genome-wide transcript analysis of *Bradyrhizobium japonicum* bacteroids in soybean root nodules. *Mol Plant-Microbe Interact* **20**: 1353-1363.

24. Yang J, Sangwan I, Lindemann A, Hauser F, Hennecke H, Fischer HM. O'Brian MR. (2006) *Bradyrhizobium japonicum* senses iron through the status of haem to regulate iron homeostasis and metabolism. *Mol Microbiol* **60**: 427-437.

25. Donati AJ, Jeon JM, Sangurdekar D, So JS, Chang WS. 2011. Genome-wide transcriptional and physiological responses of *Bradyrhizobium japonicum* to paraquat-mediated oxidative stress. *Appl Environ Microbiol* **77**: 3633-3643.

26. Wei X, Bauer WD. 1998. Starvation-induced changes in motility, chemotaxis, and flagellation of *Rhizobium meliloti*. *Appl Environ Microbiol* **64**: 1708-1714.

27. Fretin D, Fauconnier A, Kohler S, Halling S, Leonard S, Nijskens C, Ferooz J, Lestrate P, Delrue RM, Danese I, Vandenhaute J, Tibor A, DeBolle X, Letesson JJ. 2005. The sheathed flagellum of *Brucella melitensis* is involved in persistence in a murine model of infection. *Cell Microbiol* **7**: 687-698.

28. Rotter C, Muhlbacher S, Salamon D, Schmitt R, Scharf B.2006. Rem, a new transcriptional activator of motility and chemotaxis in *Sinorhizobium meliloti*. *J Bacteriol* **188**: 6932-6942.

29. Hoang HH, Gurich N, González JE. 2008. Regulation of motility by the ExpR/Sin quorum-sensing system in *Sinorhizobium meliloti*. *J Bacteriol* **190**: 861-871.

30. Althabegoiti MJ, Covelli JM, Pérez-Giménez J, Quelas JI, Mongiardini EJ, López MF, López-García SL, Lodeiro AR.2011. Analysis of the role of the two flagella of Bradyrhizobium japonicum in competition for nodulation of soybean. *FEMS Microbiol Lett* **319**: 133-139.

31. López-García SL, Perticari A, Piccinetti C, Ventimiglia L, Arias N, De Battista J, Althabegoiti MJ, Mongiardini EJ, Pérez-Giménez J, Quelas JI, Lodeiro AR. 2009. In-furrow inoculation and selection for higher motility enhances the eficacy of *Bradyrhizobium japonicum* nodulation. *Agron J* **101**: 1-7.

32. Leonard S, Ferooz J, Haine V, Danese I, Fretin D, Tibor, A., de Walque S, De Bolle X, Letesson JJ. 2007. FtcR is a new master regulator of the flagellar system of *Brucella melitensis* 16M with homologs in *Rhizobiaceae*. *J Bacteriol* **189**: 131-141.

33. Kaneko T, Nakamura Y, Sato S, Minamisawa K, Uchiumi T, Sasamoto S, Watanabe A, Idesawa K, Iriguchi M, Kawashima K, Kohara M, Matsumoto M, Shimpo S, Tsuruoka H, Wada T, Yamada M, Tabata S. 2002. Complete genomic sequence of nitrogen-fixing symbiotic bacterium *Bradyrhizobium japonicum* USDA110. *DNA Res* **9**: 189-197.

34. Čuklina J, Hahn J, Imakaev M, Omasits U, Förstner KU, Ljubimov N, Goebel M, Pessi G, Fischer HM, Ahrens CH, Gelfand MS, Evguenieva-Hackenberg E. 2016. Genome-wide transcription start site mapping of *Bradyrhizobium japonicum* grown free-living or in symbiosis -a rich resource to identify new transcripts, proteins and to study gene regulation. *BMC Genomics* **17**: 302.

35. Redondo-Nieto M, Lloret J, Larenas J, Barahona E, Navazo A, Martínez-Granero F, Capdevila S, Rivilla R, Martín M. 2008. Transcriptional organization of the region encoding the synthesis of the flagellar filament in *Pseudomonas fluorescens*. *J Bacteriol* **190**: 4106-4109.

36. Bailey TL, Elkan C. 1994. Fitting a mixture model by expectation maximization to discover motifs in biopolymers. *Proc Int Conf Intell Syst Mol Biol*. **2**:28-36.

37. Mangan EK, Malakooti J, Caballero A, Anderson P, Ely B, Gober JW. 1999. FlbT couples flagellum assembly to gene expression in *Caulobacter crescentus*. *J Bacteriol* **181**: 6160-6170.

38. Ferooz J, Lemaire J, Letesson JJ. 2011. Role of FlbT in flagellin production in *Brucella melitensis*. *Microbiology* **157**: 1253-1262.

39. Anderson PE, Gober JW. 2000. FlbT, the post-transcriptional regulator of flagellin synthesis in *Caulobacter crescentus*, interacts with the 5' untranslated region of flagellin mRNA. *Mol Microbiol* **38**: 41-52.

40. Lang AS, Beatty JT. 2002. A bacterial signal transduction system controls genetic exchange and motility. *J Bacteriol* **184**: 913-918.

41. Sourjik V, Muschler P, Scharf B, Schmitt R. 2000. VisN and VisR are global regulators of chemotaxis, flagellar, and motility genes in *Sinorhizobium* (*Rhizobium*) *meliloti*. *J Bacteriol* **182**: 782-788.

42. Tambalo DD, Del Bel KL, Bustard DE, Greenwood PR, Steedman AE, Hynes MF.2010. Regulation of flagellar, motility and chemotaxis genes in *Rhizobium leguminosarum* by the VisN/R-Rem cascade. *Microbiology* **156**: 1673-1685.

43. Thorne DW, Burris RH. 1940. Respiratory enzyme systems in symbiotic nitrogen fixation: III. The respiration of *Rhizobium* from legume nodules and laboratory cultures. *J Bacteriol* **39**: 187-196.

44. Lindemann A, Moser A, Pessi G, Hauser F, Friberg M, Hennecke H, Fischer HM. 2007. New target genes controlled by the *Bradyrhizobium japonicum* two-component regulatory system RegSR. *J Bacteriol* **189**: 8928-8943.

45. Ohkama-Ohtsu N, Honma H, Nakagome M, Nagata M, Yamaya-Ito H, Sano Y, Hiraoka N, Ikemi T, Suzuki A, Okazaki S, Minamisawa K, Yokoyama T. 2016. Growth rate of and gene expression in *Bradyrhizobium diazoefficiens* USDA110 due to a mutation in blr7984, a TetR family transcriptional regulator gene. *Microbes Environ* **31**: 249-259.

46. Herlihey FA, Moynihan PJ, Clarke AJ. 2014. The essential protein for bacterial flagella formation FlgJ functions as a beta-N-acetylglucosaminidase. *J Biol Chem* **289**: 31029-31042.

47. Llewellyn M, Dutton RJ, Easter J, O'Donnol D, Gober JW.2005. The conserved *flaF* gene has a critical role in coupling flagellin translation and assembly in *Caulobacter crescentus*. *Mol Microbiol* **57**: 1127-1142.

48. Sadowsky MJ, Tully RE, Cregan PB, Keyser HH 1987. Genetic diversity in *Bradyrhizobium japonicum* serogroup 123 and its relation to genotype-specific nodulation of soybean. *Appl Environ Microbiol* **53**:2624-2630.

49. Vincent JM. 1970. A manual for the practical study of the root nodule bacteria. IBP

handbook No. 15. Oxford: Blackwell Scientific Publications.

50. Regensburger B, Hennecke H. 1983. RNA polymerase from *Rhizobium japonicum*. *Arch Microbiol* **135**: 103-109.

51. Sambrook J, Russell D. 2001. Molecular Cloning: A Laboratory Manual, 3rd edn. New York: Cold Spring Habor Laboratory Press.

52. Sievers F, Wilm A, Dineen DG, Gibson TJ, Karplus K, Li W, Lopez R, McWilliam H, Remmert M, Söding J, Thompson JD, Higgins DG. 2011. Fast, scalable generation of high-quality protein multiple sequence alignments using Clustal Omega. *Mol Syst Biol* **7**: 539.

53. McWilliam H, Li W, Uludag M, Squizzato S, Park YM, Buso N, Cowley AP, Lopez R. 2013. Analysis Tool Web Services from the EMBL-EBI. *N Nucleic Acids Res* **41**(Web Server issue):W597-600.

54. Taboada B, Ciria R, Martínez-Guerrero CE, Merino E. 2012.ProOpDB: Prokaryotic Operon DataBase. *Nucleic Acids Res* **40**(Database issue):D627-31.

55. Mao X, Ma Q, Zhou C, Chen X, Zhang H, Yang J, Mao F, Lai W, Xu Y. 2014. DOOR 2.0: presenting operons and their functions through dynamic and integrated views. *Nucleic Acids Res* **42**(Database issue):D654-9.

56. Dehal PS, Joachimiak MP, Price MN, Bates JT, Baumohl JK, Chivian D, Friedland GD, Huang KH, Keller K, Novichkov PS, Dubchak IL, Alm EJ, Arkin AP. 2010. MicrobesOnline: an integrated portal for comparative and functional genomics. *Nucleic Acids Res* **38**(Database issue):D396-400.

57. Freese NH, Norris DC, Loraine AE. 2016. Integrated genome browser: visual analytics platform for genomics. *Bioinformatics* **32**:2089-2095.

58. Ye J, Coulouris G, Zaretskaya I, Cutcutache I, Rozen S, Madden T. 2012. Primer-BLAST: A tool to design target-specific primers for polymerase chain reaction. *BMC Bioinformatics* **13**: 134.

59. Zuker M. 2003. Mfold web server for nucleic acid folding and hybridization prediction. *Nucleic Acids Res* **31**: 3406-3415.

60. Crooks GE, Hon G, Chandonia JM, Brenner SE. 2004. WebLogo: A sequence logo generator. *Genome Res* **14**: 1188-1190.

61. Quelas JI, Mongiardini EJ, Casabuono A, López-García SL, Althabegoiti MJ, Covelli JM, Pérez-Giménez J, Couto A, Lodeiro AR. 2010. Lack of galactose or galacturonic acid in *Bradyrhizobium japonicum* USDA 110 exopolysaccharide leads to different symbiotic responses in soybean. *Mol. Plant-Microbe Interact*. **23**:1592-1604.

62. Kirchner O, Tauch A. 2003. Tools for genetic engineering in the amino acid-producing bacterium *Corynebacterium glutamicum*. *J Biotechnol* **104**: 287-299.

63. Vieira J, Messing J.1982. The pUC plasmids, an M13mp7-derived system for insertion mutagenesis and sequencing with synthetic universal primers. *Gene* **19**: 259-68.

64. Schäfer A, Tauch A, Jäger W, Kalinowski J, Thierbach G, Pühler A.1994. Small mobilizable multi-purpose cloning vectors derived from the *Escherichia coli* plasmids pK18 and pK19: selection of defined deletions in the chromosome of *Corynebacterium glutamicum*. *Gene* **145**: 69-73.

65. Link AJ, Phillips D, Church GM. 1997. Methods for generating precise deletions and insertions in the genome of wild-type *Escherichia coli*: application to open reading frame characterization. *J Bacteriol* **179**:6228-6237.

66. Dombrecht B, Vanderleyden J, Michiels J. 2001. Stable RK2-derived cloning vectors for the analysis of gene expression and gene function in gram-negative bacteria. *Mol Plant-Microbe Interact.* **14**: 426-430.

67. Schneider K, Beck CF. 1987. New expression vectors for identifying and testing signal structures for initiation and termination of transcription. *Methods Enzymol* **153**: 452-461.

68. Hauser F, Lindemann A, Vuilleumier S, Patrignani A, Schlapbach R, Fischer H-M, Hennecke H. 2006. Design and validation of a partial-genome microarray for

transcriptional profiling of the *Bradyrhizobium japonicum* symbiotic gene region. *Mol Genet Genomics* **275**: 55-67

69. Laemmli UK. 1970. Cleavage of structural proteins during the assembly of the head of bacteriophage T4. *Nature* **227**:680-685.

70. Pérez-Giménez J, Covelli JM, López MF, Althabegoiti MJ, Ferrer-Navarro M, Mongiardini EJ, Lodeiro AR. 2012. Soybean seed lectin prevents the accumulation of S-adenosyl methionine synthetase and the S1 30S ribosomal protein in *Bradyrhizobium japonicum* under C and N starvation. *Curr Microbiol* **65**: 465-474.

FIGURE LEGENDS

Fig. 1. *Control of flagellin expression and motility by* lafR *in bacteria grown in liquid HMY with arabinose (Ara) or mannitol (Man) as carbon source*

A. SDS-PAGE of extracellular *Bradyrhizobium diazoefficiens* proteins of the subpolar flagellins (FliC, upper bands) and lateral flagellins (LafA, lower bands) in the wild-type (WT) and the *lafR*::Km extracts alone, or in extracts from the WT and the *lafR*::Km strains complemented with a WT copy of *lafR* under the direction of the *nptII* promoter (pFAJ::*lafR*)

B. Agarose gel of RNA retrotranscripts amplified by RT-PCR of *lafR* in the WT or the *lafR*::Km mutant with the primers indicated in Fig. S2B and listed in Table S2, compared with *sigA* as constitutive reference gene. A PCR from genomic DNA was performed as positive control (+C).

C. Swimming motility in 0.3% (w/v) agar-containing AG medium. Left: the wild-type (WT) compared to the mutants *lafR*::Km, $\Delta flbT_L$, and Δ*lafA*, this last lacking lateral flagellins. Center: complementation of motility in the *lafR*::Km mutant with the pFAJ::*lafR* plasmid in comparison to the *lafR*::Km mutant carrying empty vector (pFAJ), or *lafR*::Km mutant carrying pFAJ::$flbT_L$. Right: complementation of motility in the $\Delta flbT_L$ with the pFAJ::$flbT_L$ plasmid in comparison with $\Delta flbT_L$ carrying the empty vector (pFAJ). The results of all the complementations may be compared to the motility of the WT carrying the empty vector (WT pFAJ, right).

D. SDS-PAGE of the *B. diazoefficiens* extracellular proteins—the subpolar flagellins (FliC, upper bands) and lateral flagellins (LafA, lower bands)—in the wild-type (WT) and the *lafR* point mutants D50A (with the Asp50 residue replaced by an Ala), D50G (the Asp50 replaced by a Gly), and D50E (the Asp50 replaced by a Glu).

E. Composite SDS-PAGE of the subpolar (FliC, upper bands) and lateral (LafA, lower bands) flagellins of *B. diazoefficiens* or the FlaA-D flagellins of *E. meliloti* (Fla, middle bands). The flagellins are from the *B. diazoefficiens* (*Bd*) wild-type (WT) and the *lafR*::Km mutant either alone or complemented with pFAJ::*lafR* or with a wild-type copy of *rem* under the *nptII* promoter (pFAJ::*rem*), wild-type *E. meliloti* (*Em* WT), and the *E. meliloti rem* mutant (Δ*rem*) either alone or complemented with pFAJ::*rem* or pFAJ::*lafR*. All the bacteria were grown on HMY with arabinose as the carbon source. The gels were run simultaneously in the same equipment.

Fig. 2. *Operons of the lateral-flagellar–gene cluster, indicating the transcription directions according to* Rhizobase (http://genome.annotation.jp/rhizobase/Bradyrhizobium).

A. The genes identified in the cluster are classified by function as: regulators (R, gray), unknown (?, white), hook and hook-filament junction (H and HJ, violet), export apparatus (EA, green), motor (M, orange), MS ring (pink), flagellins (F, red), basal body (B, blue), L-ring and P-ring (LRi and PRi, turquoise), distal and proximal rods (Dr and Pr, light blue), and C-ring (CR, light pink). Below this scheme, the operon structure is indicated according to: bioinformatics prediction (upper light-pink line), Čuklina *et al.*, 2016 (34) (middle light-pink line), and our results from RT-PCR (bottom light-pink line). Above the scheme, the positions of the deduced *lafR*-dependent promoters are shown as black arrows, and the positions of the intergenic amplicons predicted according to the RT-PCR strategy outlined in Fig. S4 are shown as black segments numbered from 1 to 8. For the sake of simplicity, in the figure, the L subscripts have been omitted from the name of each locus.

B. Sequence alignment of the conserved motifs found upstream from the transcription start sites (designated as +1) of the genes *motA* (**a**), $fliF_L$ (**b**), $flgF_L1$ (**c**), the latter being located at the 5' ends of operons I, II, and III, respectively (Panel **A**). The consensus sequence that may be deduced is indicated below.

Fig.3. *Effects of mutations in* lafR *and* $flbT_L$ *on the mRNA accumulation of selected lateral-flagellar genes.*

A. Transcription-expression level in the wild-type (WT) strain relative to that of the *lafR*::Km mutant ± SD, as determined by qRT-PCR from at least three independent biological replicas for the indicated genes (locus tags), the latter being representative of the different transcriptional units. Mono.: monocistronic transcripts. *The relative expression of *lafR* was evaluated with the primers indicated in Fig. S2B, which amplify the 5' end of *lafR* both in the wild-type and in the *lafR*::Km mutant. Stars: statistically significant differences (p <0.05) from a threshold interval 0.5-2.0 according to the Student´s t test.

B. Transcription-expression level in the wild-type (WT) strain relative to that of $\Delta flbT_L$ ($LafR^+/FlbT_L^-$, left) or that of *lafR*::Km carrying the plasmid pFAJ::$flbT_L$ ($LafR^-/FlbT_L^C$, right) ± SD, as determined by qRT-PCR from at least three independent biological replicas for the indicated genes, the latter having been selected to indicate the differential influence of $flbT_L$ on *lafA1* expression. Stars: statistically significant differences (p <0.05) from a threshold interval 0.5-2.0 according to the Student´s t-test.

For the sake of simplicity, in the figure, the L subscripts have been omitted from the name of each locus.

Fig.4. *Control of flagellin expression by* $flbT_L$ *in bacteria grown in liquid HMY medium with arabinose (Ara) or mannitol (Man) as carbon source*

A. SDS-PAGE of the *B. diazoefficiens* extracellular subpolar (FliC) and lateral (LafA) flagellins in the wild-type (WT), the $\Delta flbT_L$ strain, the $\Delta flbT_L$ strain complemented with the plasmid pFAJ:: $flbT_L$ that carries a wild-type copy of $flbT_L$ under the direction of the *nptII* promoter, or the *lafR*::Km strain complemented with the plasmid pFAJ:: $flbT_L$ or pFAJ::*lafR*.

B. Western blots of the cellular *B. diazoefficiens* proteins FliC and LafA, as visualized by an anti-*lafA* polyclonal antiserum, from the wild-type (WT) strain either alone or complemented with the plasmid pFAJ::*flbT*$_L$, or from the *lafR*::Km strain complemented with the plasmid pFAJ:: *flbT*$_L$. The polyclonal anti-*lafA* serum exhibited some cross-reaction against FliC, which activity in this experiment served as internal standard.

Fig. 5. *β-Galactosidase activities of the pCB::P*lafA1 *and pCB::P*lafA2 lacZ *fusions within three genetic backgrounds.*

In the figure, the β-galactosidase activity in Miller units is plotted on the *ordinate* for each of the genetic backgrounds denoted on the *abscissa*. The two clonal fusions are indicated in brackets below the figure. Each mean value is from two independent clones measured in duplicate. Error bars are standard deviations.

Fig. 6. *Scheme of the regulation of the lateral-flagellar genes that may be deduced from the present results.*

Cultivation with arabinose as the carbon source induces the expression of *lafR*, whereas cultivation with mannitol as the carbon source does not. LafR activates the transcription (Txn) of operons I, II, and III without any special hierarchical order among them, while the monocistronic *lafA2* is transcribed independently of LafR. Operon I contains *flbT*$_L$; which locus, upon activation, acts as a translation (Tln) inducer of the monocistronic *lafA2* and appears to stabilize (Stb) the *lafA1* transcript from a promoter within Operon II. In addition to the effects of arabinose and mannitol, evidence from the literature indicates that prolonged exposure to moderate oxidative stress also induces *lafR* and the lateral flagellar regulon (25), whereas situations of O_2 limitation as the bacteroid state (23) or iron-limitation (24) repress them. We also observed that viscosity and tortuousity of the medium induce lateral flagella (20), and microoxia was reported as inhibiting lateral flagella genes expression (23). Therefore, the signal to which the expression of lateral-flagellar genes responds might be related to the energy status of the cell, apart from the specific carbon source available.

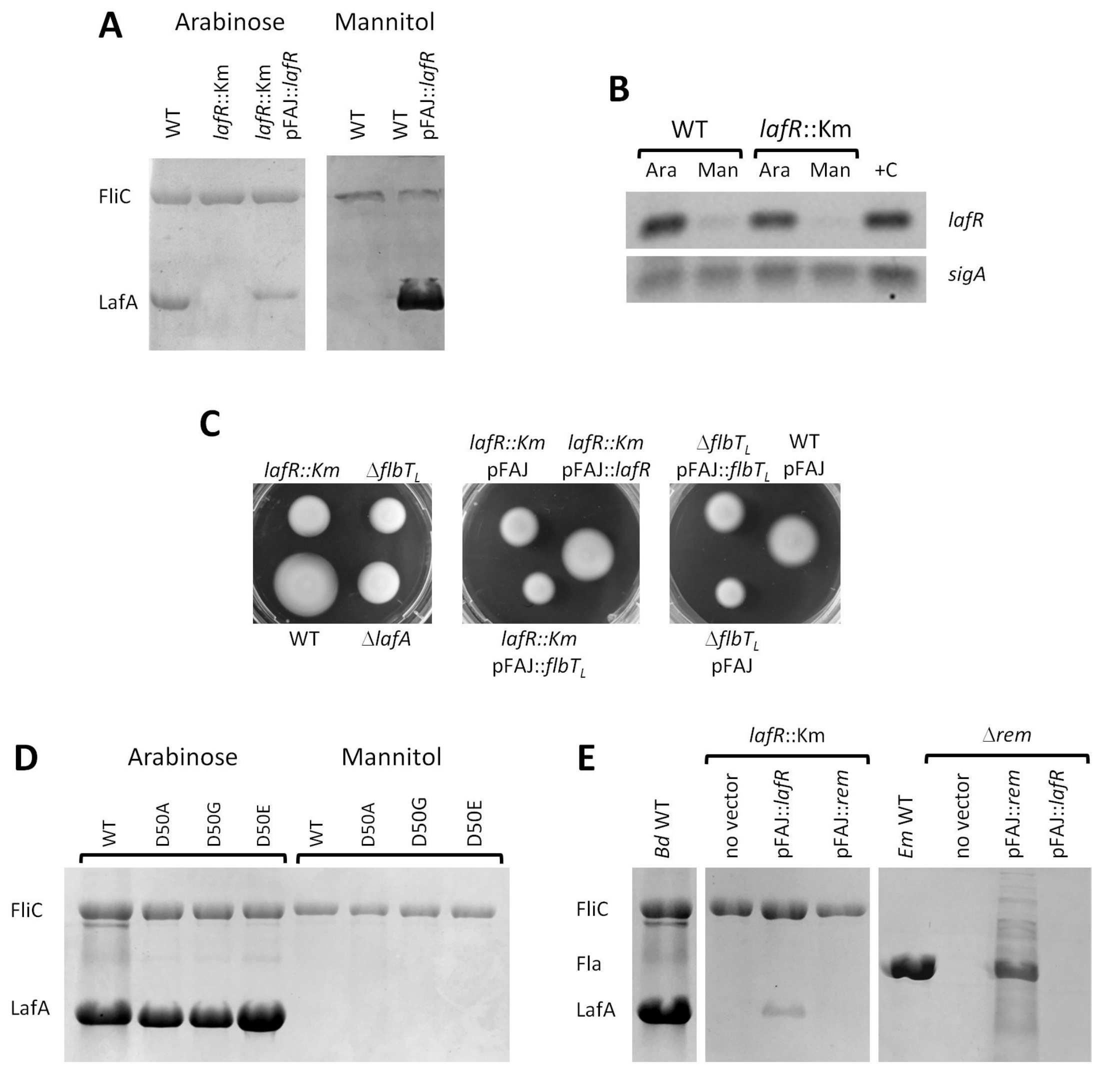
A
Arabinose
Mannitol
WT
lafR::Km
lafR::Km pFAJ::lafR
WT
WT pFAJ::lafR
FliC
LafA
B
WT
lafR::Km
Ara
Man
Ara
Man
+C
lafR
sigA
C
lafR::Km
ΔflbT_L
WT
ΔlafA
lafR::Km pFAJ
lafR::Km pFAJ::lafR
lafR::Km pFAJ::flbT_L
ΔflbT_L pFAJ::flbT_L
WT pFAJ
ΔflbT_L pFAJ
D
Arabinose
Mannitol
WT
D50A
D50G
D50E
WT
D50A
D50G
D50E
FliC
LafA
E
lafR::Km
Δrem
Bd WT
no vector
pFAJ::lafR
pFAJ::rem
Em WT
no vector
pFAJ::rem
pFAJ::lafR
FliC
Fla
LafA

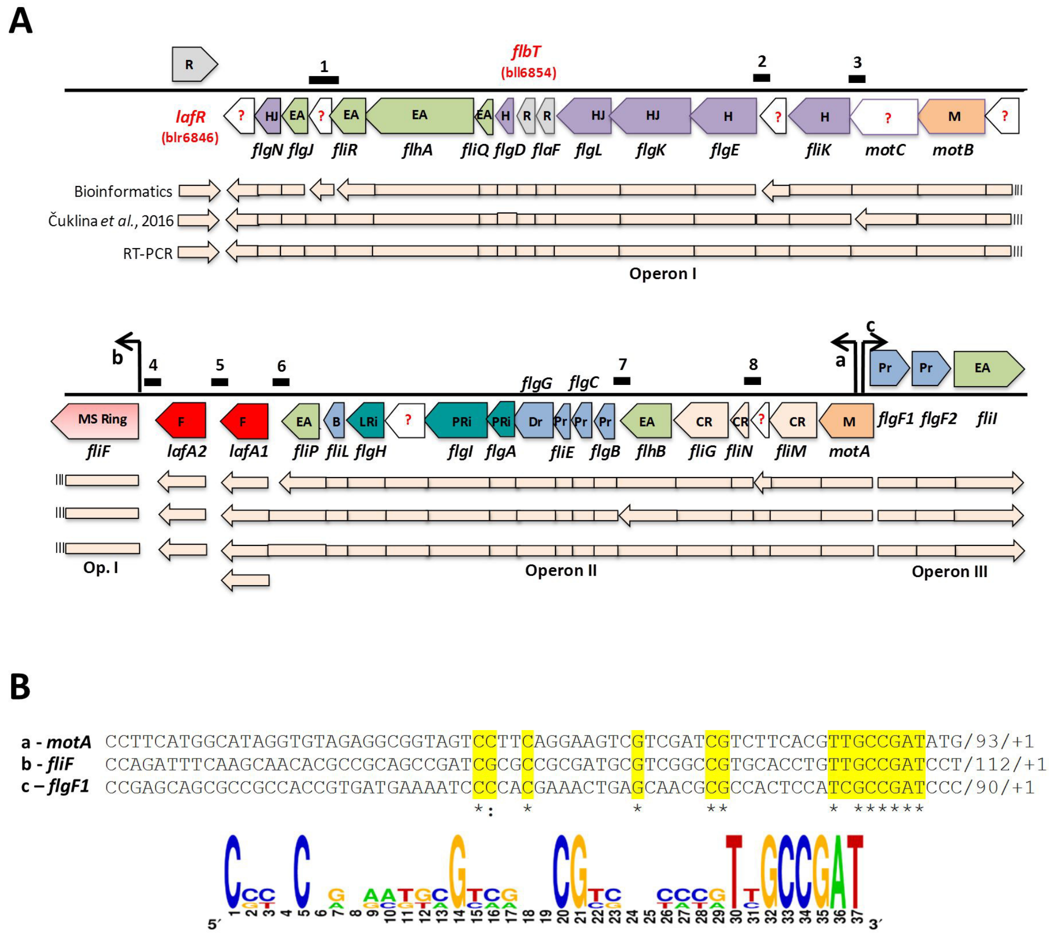
A
R
flbT
(bll6854)
lafR
(blr6846)
flgN flgJ fliR flhA fliQ flgD flaF flgL flgK flgE fliK motC motB
Bioinformatics
Čuklina et al., 2016
RT-PCR
Operon I
fliF lafA2 lafA1 fliP fliL flgH flgI flgA fliE flgB flhB fliG fliN fliM motA flgF1 flgF2 fliI
flgG flgC
Op. I
Operon II
Operon III
B
a - motA CCTTCATGGCATAGGTGTAGAGGCGGTAGTCCTTCAGGAAGTCGTCGATCGTCTTCACGTTGCCGATATG/93/+1
b - fliF CCAGATTTCAAGCAACACGCCGCAGCCGATCGCGCCGCGATGCGTCGGCCGTGCACCTGTTGCCGATCCT/112/+1
c – flgF1 CCGAGCAGCGCCGCCACCGTGATGAAAATCCCCACGAAACTGAGCAACGCGCCACTCCATCGCCGATCCC/90/+1

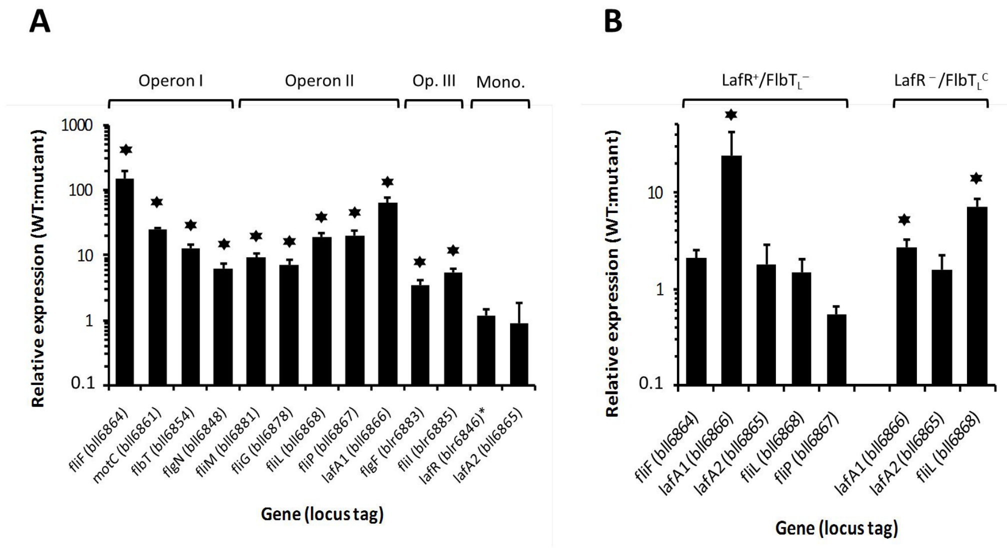
A
Operon I
Operon II
Op. III
Mono.
Relative expression (WT:mutant)
1000
100
10
1
0.1
fliF (bll6864)
motC (bll6861)
flbT (bll6854)
flgN (bll6848)
fliM (bll6881)
fliG (bll6878)
fliL (bll6868)
fliP (bll6867)
lafA1 (bll6866)
flgF (blr6883)
fliI (blr6885)
lafR (blr6846)*
lafA2 (bll6865)
Gene (locus tag)
B
LafR+/FlbTL−
LafR−/FlbTLC
Relative expression (WT:mutant)
10
1
0.1
fliF (bll6864)
lafA1 (bll6866)
lafA2 (bll6865)
fliL (bll6868)
fliP (bll6867)
lafA1 (bll6866)
lafA2 (bll6865)
fliL (bll6868)
Gene (locus tag)

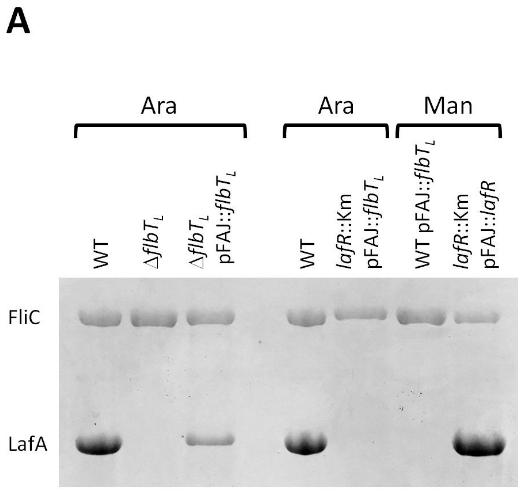
A
Ara
Ara
Man
WT
ΔflbT$_L$
ΔflbT$_L$ pFAJ::flbT$_L$
WT
lafR::Km pFAJ::flbT$_L$
WT pFAJ::flbT$_L$
lafR::Km pFAJ::lafR
FliC
LafA

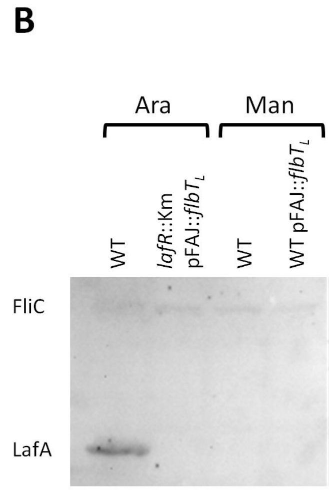
B
Ara
Man
WT
lafR::Km pFAJ::flbT$_L$
WT
WT pFAJ::flbT$_L$
FliC
LafA

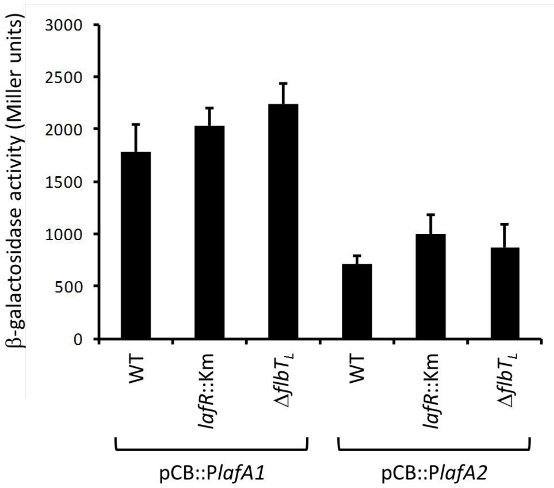
β-galactosidase activity (Miller units)
3000
2500
2000
1500
1000
500
0
WT
lafR::Km
ΔflbT_L
WT
lafR::Km
ΔflbT_L
pCB::PlafA1
pCB::PlafA2

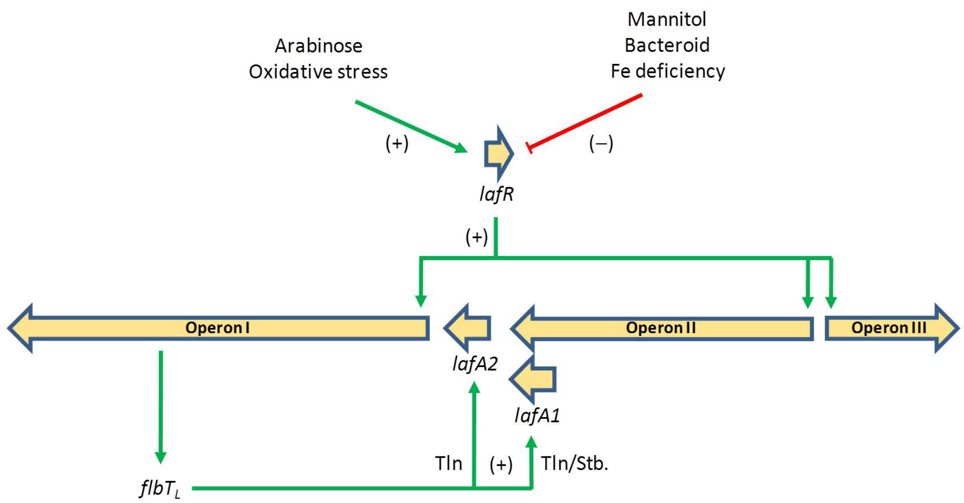
Arabinose
Oxidative stress
Mannitol
Bacteroid
Fe deficiency
(+)
(–)
lafR
(+)
Operon I
Operon II
Operon III
lafA2
lafA1
Tln
(+)
Tln/Stb.
flbT_L